AD-A056 822 ITEK CORP LEXINGTON MASS OPTICAL SYSTEMS DIV F/G 20/3
DIELECTRIC AND OPTICAL PROPERTIES OF THIN FILMS.(U)
AUG 78 R E ALDRICH, S C MORENO DAAG29-77-C-0027
UNCLASSIFIED PFR-78-040 ARO-15216.1-P NL

1 OF 1
AD A056822

END
DATE FILMED
9-78
DDC

LEVEL II

ARO 15216.1-P

(12)

Report DAAG29-77-C-0027

DIELECTRIC AND OPTICAL PROPERTIES OF THIN FILMS

FINAL REPORT
AUGUST 1978

Prepared by
ITEK CORPORATION
OPTICAL SYSTEMS DIVISION
10 MAGUIRE ROAD
LEXINGTON, MASSACHUSETTS 02173

UNDER CONTRACT: DAAG29-77-C-0027
DATE OF CONTRACT: JULY 1977

Principal Investigator: Dr. Ralph E. Aldrich (617) 276-2157
Project Engineer: Salvatore C. Moreno (617) 276-2902

Prepared for
U.S. Army Research Office
Box 12211
Research Triangle Park, North Carolina 27709

Report DAAG29-77-C-0027

DIELECTRIC AND OPTICAL PROPERTIES OF THIN FILMS

FINAL REPORT
AUGUST 1978

Prepared by
ITEK CORPORATION
OPTICAL SYSTEMS DIVISION
10 MAGUIRE ROAD
LEXINGTON, MASSACHUSETTS 02173

UNDER CONTRACT: DAAG29-77-C-0027
DATE OF CONTRACT: JULY 1977

Principal Investigator: Dr. Ralph E. Aldrich (617) 276-2157
Project Engineer: Salvatore C. Moreno (617) 276-2902

Prepared for
U.S. Army Research Office
Box 12211
Research Triangle Park, North Carolina 27709

UNCLASSIFIED

SECURITY CLASSIFICATION OF THIS PAGE *(When Data Entered)*

REPORT DOCUMENTATION PAGE

READ INSTRUCTIONS BEFORE COMPLETING FORM

1. REPORT NUMBER: ~~DAAG29-77-C-0027~~
2. GOVT ACCESSION NO.
3. RECIPIENT'S CATALOG NUMBER

4. TITLE *(and Subtitle)*: DIELECTRIC AND OPTICAL PROPERTIES OF THIN FILMS
5. TYPE OF REPORT & PERIOD COVERED: Final Report: 15 JUL 77 - 14 JUL 78
6. PERFORMING ORG. REPORT NUMBER: PFR-78-040

7. AUTHOR(s): Ralph E. Aldrich; Salvatore C. Moreno
8. CONTRACT OR GRANT NUMBER(s): DAAG29-77-C-0027

9. PERFORMING ORGANIZATION NAME AND ADDRESS:
Itek Corporation
10 Maguire Road
Lexington, Massachusetts 02173

10. PROGRAM ELEMENT, PROJECT, TASK AREA & WORK UNIT NUMBERS

11. CONTROLLING OFFICE NAME AND ADDRESS:
U.S. Army Research Office
Box 12211
Research Triangle Park, North Carolina 27709

12. REPORT DATE: Aug 1978
13. NUMBER OF PAGES: 36 P.

14. MONITORING AGENCY NAME & ADDRESS *(if different from Controlling Office)*: ITRC 15216.1-P

15. SECURITY CLASS. *(of this report)*: Unclassified

15a. DECLASSIFICATION/DOWNGRADING SCHEDULE

16. DISTRIBUTION STATEMENT *(of this Report)*

Approved for public release; distribution unlimited.

17. DISTRIBUTION STATEMENT *(of the abstract entered in Block 20, if different from Report)*

18. SUPPLEMENTARY NOTES

THE VIEW, OPINIONS, AND/OR FINDINGS CONTAINED IN THIS REPORT ARE THOSE OF THE AUTHOR(S) AND SHOULD NOT BE CONSTRUED AS AN OFFICIAL DEPARTMENT OF THE ARMY POSITION, POLICY, OR DECISION, UNLESS SO DESIGNATED BY OTHER DOCUMENTATION.

19. KEY WORDS *(Continue on reverse side if necessary and identify by block number)*

Dielectrics, Thin Films

20. ABSTRACT *(Continue on reverse side if necessary and identify by block number)*

For several years, Itek Corporation has been developing an electro-optic imaging device, the Itek PROM (Pockels Readout Optical Modulator). The device required an insulating layer, which acts with an electro-optic photoconductor to provide a voltage division that is detectable through the Pockels effect. The original insulating layer was Parylene C, a vapor-deposited linear polymer. The purpose of this paper is to identify other insulating or blocking layers that possess higher dielectric constants and greater breakdown fields, are more durable, and are capable of being vacuum evaporated. The materials investigated were

DD FORM 1 JAN 73 1473 EDITION OF 1 NOV 65 IS OBSOLETE

464 157

UNCLASSIFIED

SECURITY CLASSIFICATION OF THIS PAGE *(When Data Entered)*

20. ABSTRACT

SiO_2, Al_2O_3, Ta_2O_5, ZrO_2 and TiO_2. Also during the program, multilayer evaporations of TiO_2/SiO_2, Ta_2O_5/SiO_2, ZrO_2/SiO_2, and HfO_2/SiO_2 were investigated as dielectrics. In addition, an In_2O_3/SnO_2 coating was studied as a transparent, conductive, vacuum-evaporated film. The optical and electrical properties of these coatings are discussed with respect to their use with the Itek PROM.

ABSTRACT

For several years, Itek Corporation has been developing an electro-optic imaging device, the Itek PROM (Pockels Readout Optical Modulator). The device required an insulating layer, which acts with an electro-optic photoconductor to provide a voltage division that is detectable through the Pockels effect. The original insulating layer was Parylene C, a vapor-deposited linear polymer. The purpose of this paper is to identify other insulating or blocking layers that possess higher dielectric constants and greater breakdown fields, are more durable, and are capable of being vacuum evaporated. The materials investigated were SiO_2, Al_2O_3, Ta_2O_5, ZrO_2 and TiO_2. Also during the program, multilayer evaporations of TiO_2/SiO_2, Ta_2O_5/SiO_2, ZrO_2/SiO_2, and HfO_2/SiO_2 were investigated as dielectrics. In addition, an In_2O_3/SnO_2 coating was studied as a transparent, conductive, vacuum-evaporated film. The optical and electrical properties of these coatings are discussed with respect to their use with the Itek PROM.

CONTENTS

FIGURES

TABLES

1. INTRODUCTION

A great deal of literature has been published on the properties of semiconductors, and on the processes governing these properties. However, similar data on dielectrics as dielectrics is not readily available. Some data is available on materials that have been studied as thin film capacitors, but this information is neither complete nor definitive. The object of this program is to extend the available data on dielectrics for one specific purpose: the dielectric coatings required for a Pockels Readout Optical Modulator (PROM*) device.

The PROM requires an insulating (dielectric) layer that acts with an electro-optic photoconductor to provide a voltage division. This voltage division is detectable through the Pockels effect. The usual insulating layer is Parylene C†, a vapor-deposited linear polymer that can be condensed on a room temperature substrate as a conformal coating. Optical transmission of Parylene C is excellent, its breakdown field is relatively high (5×10^6 V/cm^{-1}) for coatings 5 to 8 micrometers, and its plasticity is compatible with the large thermal expansion coefficient of the $Bi_{12}SiO_{20}$ substrate for $Bi_{12}SiO_{20}$, the thermal expansion coefficient is 1.7×10^{-5}).‡

The present program is a study of dielectric coatings that could be used as alternatives to Parylene C. Because the thickness of the dielectric coating must be monitored accurately, only vacuum deposited layers are considered. In addition to having precisely controllable thickness, the materials must be transparent to all visible wavelengths, and have reasonable deposition conditions and high breakdown field strengths. Also, they must adhere to the $B_{12}SiO_{20}$ surface.

1.1 PROM OPERATION

For several years, Itek Corporation has been developing the PROM as an electro-optic imaging device. The Itek PROM is a real-time optical storage device that can be illuminated with light from an image or a laser recorder, read out with coherent light, and erased.§ This entire sequence of operations can be completed in a very short time, making the PROM an attractive device for optical processing.

Figure 1-1 shows the configuration of a typical PROM. The device is constructed from a thin slice of bismuth silicon oxide,¶ a cubic crystal exhibiting the Pockels effect. The crystal also is photoconductive when illuminated with blue light, and has sufficient dark resistivity to allow up to 2 hours of image storage. This crystal is polished flat, coated with an insulating layer of parylene, and overcoated with transparent conducting electrodes.

*This should not be confused with the PROM (Programmable Read Only Memory) device used in the computer field.

†Trademark of Union Carbide Corporation.

‡S. Daigneault, private communication.

§D.S. Oliver et al., Appl. Phys. Lett. 17, 416 (1970).

¶R.E. Aldrich, S.L. Hou, and M.L. Haverill, J. Appl. Phys. 42, 492 (1971).

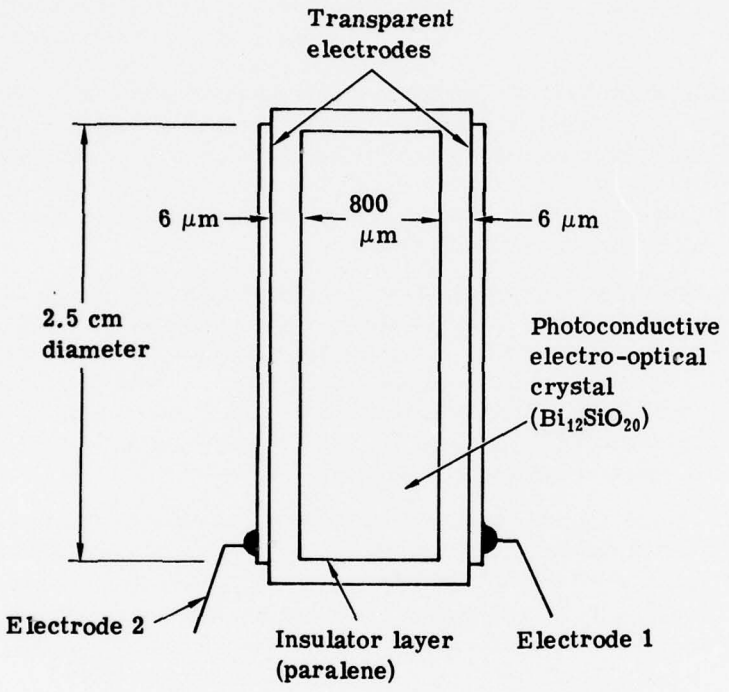

Figure 1-1 — Composition and typical dimensions of PROM

The standard operating mode for the PROM is shown in Figure 1-2. A voltage v_0 is first applied between the electrodes at a time when the crystal is fully insulating (Figure 1-2a). The PROM is then flooded with light, creating mobile electrons which drift to the crystal-Parylene interfaces until the electric field in the crystal has been cancelled (Figure 1-2b). This erases the image. The applied voltage is then reversed, resulting in a voltage approaching 2 v_0 appearing across the crystal. This voltage across the crystal is equal to the sum of applied voltage and the voltage due to stored charges (Figure 1-2c). Any point on the PROM can then be exposed to blue light, resulting in decay of the stored field at that point (Figure 1-2d). The resulting voltage pattern image is then read out with red light via the Pockels effect. Figure 1-3 shows the configuration for readout: when the PROM is placed between crossed polarizers, the amount of light passing through the second polarizer from any point on the crystal depends on the voltage at that point. Readout is done in reflection or in transmission. In the former case, a dichroic layer is added to the crystal, which reflects the red readout light. Because the device is relatively insensitive to red light, substantial energy is available for readout without destroying the stored voltage pattern. Subsequently, the applied voltage can be varied (Figures 1-2e and 1-2f) to create either a positive or negative image, or any point in between. This is possible because the transfer curve (Figure 1-4) for the linear electro-optic effects follows the relationship,

$$I_{in} = I \sin^2\left(\frac{\pi n^3 r_{41} V}{\lambda}\right) \tag{1-1}$$

where I = incident readout intensity at a wavelength λ.

n = refractive index of the $Bi_{12}SiO_{20}$ wafer at the readout wavelength

r_{41} = longitudinal linear electro-optic coefficient of the $Bi_{12}SiO_{20}$ wafer at the readout wavelength

V = total voltage across the crystal at any point.

Recently Donjon et al* showed that the modulation, m, of devices of this type is related to the capacitance of the blocking layer. Manipulating their equations, it can be shown that there is a cutoff spatial frequency, f_c, such that for $f \ll f_c$, $m \approx 1$, and for $f \gg f_c$, $m = k/f$, where k is a constant. Appendix B details this calculation.†

The expression for f_c is

$$f_c = \frac{\frac{\xi_p}{\xi_\beta} + \frac{t_p}{t_b}}{2\pi \left(\frac{\xi_p}{\xi_\beta} + 1\right) t_p} \tag{1-2}$$

where ξ_p = dielectric constant of the dielectric layer

ξ_β = dielectric constant of the electro-optic photoconductor

t_p = thickness of the dielectric layer

t_b = thickness of the electro-optic photoconductor

*J. Donjon, M. Decaesteker, B. Monod, and K. Petit, Acta Elec., 18:187 (1975)

†B. Horwitz, unpublished data, 1976.

Using typical values for a PROM composed of a $Bi_{12}SiO_{20}$ wafer ($\xi_\beta = 56$, $t_\beta = 0.8$ millimeter) coated with Parylene C ($\xi_p \cong 3$, $t_p = 6.5 \times 10^{-3}$ millimeter), a value of $f_c = 1.4$ cycle/mm is obtained. This means that all practical spatial frequencies, operation of the PROM occurs in the 1/f region of the MTF curve.

It is desirable for a variety of reasons to have an MTF that is flat over a reasonable range of spatial frequencies. Most particularly, the modulation and sensitivity of the device are uniform. Based on Equation 1-2, this can be accomplished either by reducing t_p or by increasing ξ_p. The basic accuracy of the equation was demonstrated on Itek IR&D using Parylene layers of various thicknesses.

1.2 ADVANTAGES OF THIN OXIDE DIELECTRICS

At least three improvements can be achieved in PROM devices by replacing the Parylene C dielectric with a thin oxide coating. First, thin oxide coatings may improve the PROM's resistance to humidity and ultraviolet light. Second, a think oxide coating dielectric has the potential to improve the signal-to-noise ratio of the PROM. Third, the thicknesses of the oxide coatings can be controlled precisely to improve the optical efficiency of the PROM.

1.2.1 Improved Resistance to Humidity and Ultraviolet Light

Replacing Parylene C with an oxide coating as a blocking layer eliminates the severe problem of dielectric breakdown field sensitivity to humidity (see Figure 1-5). It also eliminates the problems associated with chemical degradation of the Parylene C layer caused by exposure to ultraviolet light. It has been shown that the combination of high humidity and exposure to ultraviolet light can cause failure of the Parylene C blocking layer in a matter of hours. For this reason, PROMs are specified for operation only when relative humidity is less than 60 percent, and wavelengths are longer than 400 millimeters.

1.2.2 Improved Signal-to-Noise Ratio

As Figure 1-6 and Figure 1-7 show, thin oxide coatings have the ability to improve the PROM's signal-to-noise ratio. The traces shown in Figure 1-6 were made using a Parylene-coated PROM. The lower lines show the noise signal present when the device is completely erased. The upper curves show the signal (including noise) read out after the PROM was exposed to a 108 1p/mm sinusoidal grating. (Note that the dc levels of these signals have been adjusted arbitrarily to separate them on the graph.) The important factor is that the peak-to-peak signal amplitude is only about twice the peak-to-peak noise amplitude. Compare this result with the traces shown in Figure 1-7, which were taken from a PROM coated with a crudely sputtered SiO_2 layer. Signal amplitude at 108 1p/mm is comparable, but the noise level has been reduced approximately tenfold over the Parylene-coated device. A direct comparison of the relative noise levels is shown in Figure 1-8, where the source/detector noise and the noise in the two coatings are displayed on the same plot. As in Figure 1-6 and Figure 1-7, the dc level is arbitrary. The improvement in the signal-to-noise ratio resulting from the use of an SiO_2 blocking layer is obvious.

1.2.3 Improving Optical Efficiency

Because thin oxide coatings have controlled optical thicknesses, they allow antireflection coatings and dichroic reflectors to be used to improve the optical efficiency of the device. These coatings and reflectors would also eliminate multiple reflections in the various layers. The Parylene-coated device has approximately 20 percent reflectivity loss at each face, but proper antireflection coatings should reduce this level to 1 to 3 percent, depending on the optical properties of the blocking layer. Because each blocking layer requires a different coating design, it is not possible to show actual curves here.

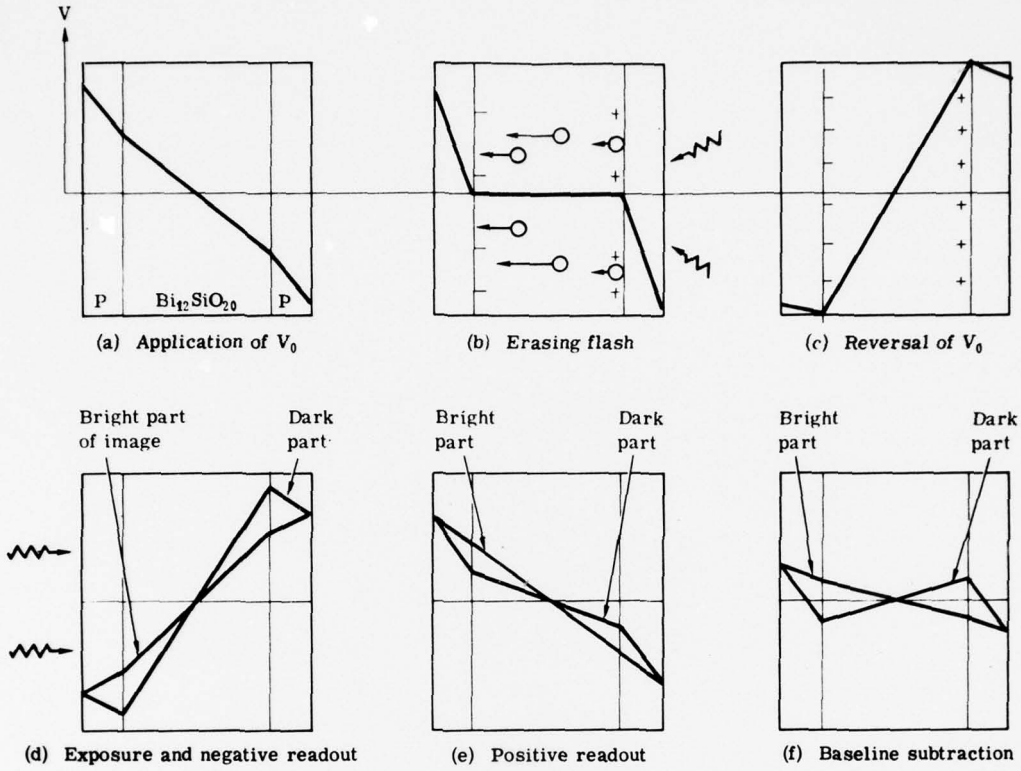

Figure 1-2 — Voltage cycle used to operate PROM

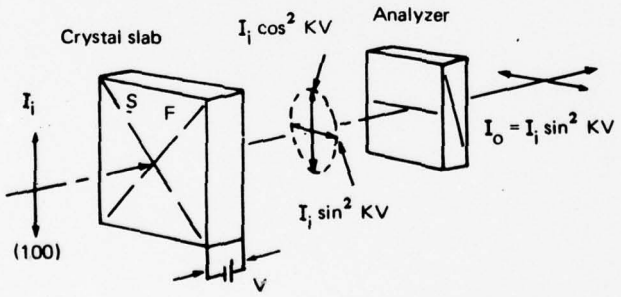

Figure 1-3 — PROM readout using Pockel effect

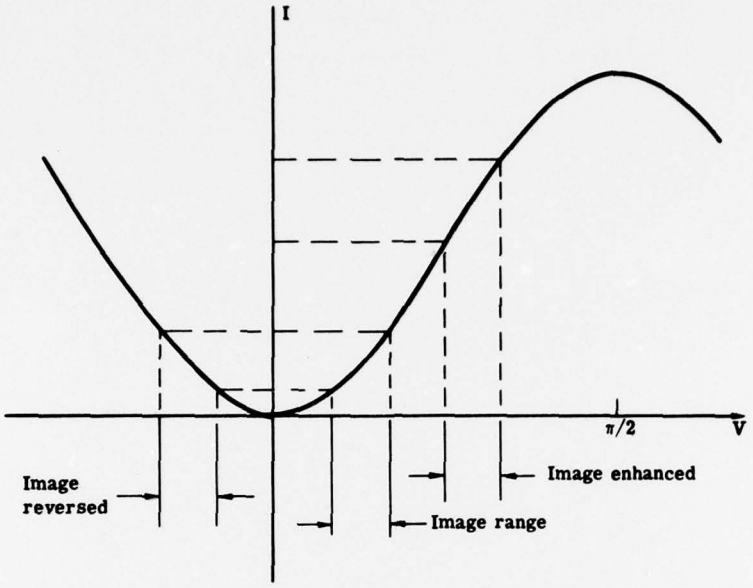

Figure 1-4 — Transfer function for the electro-optic effect

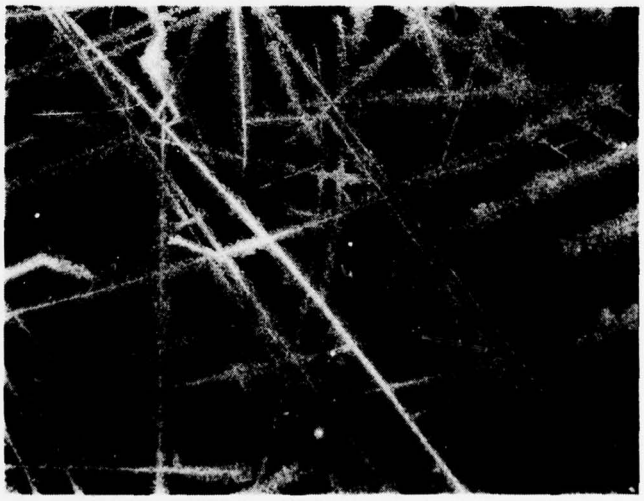

Figure 1-5 — Parylene coating on front side of PROM exposed to UV light and high humidity

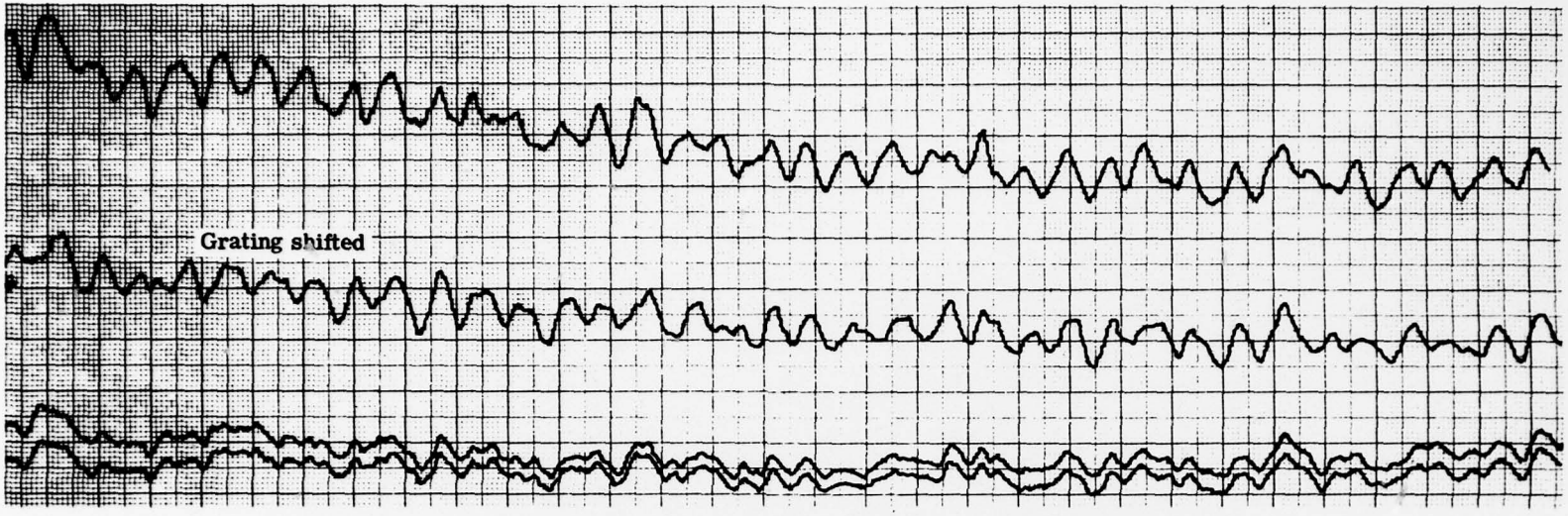

108 cycles/mm (two traces)

Figure 1-6 — Recovered signal scans with background noise—Q2-23 (108 cycles per millimeter)

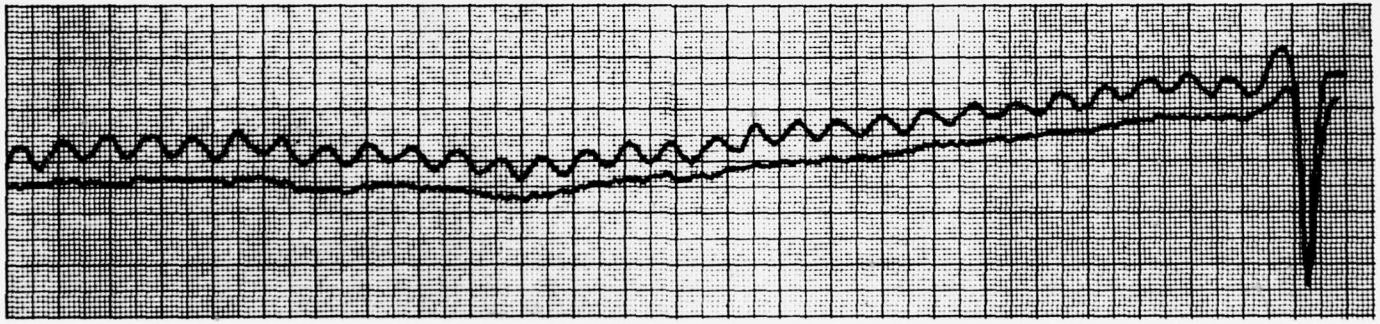

108 cycles/mm

Figure 1-7 — Recovered signal scans with background noise—SiO_2 PROM (108 cycles per millimeter)

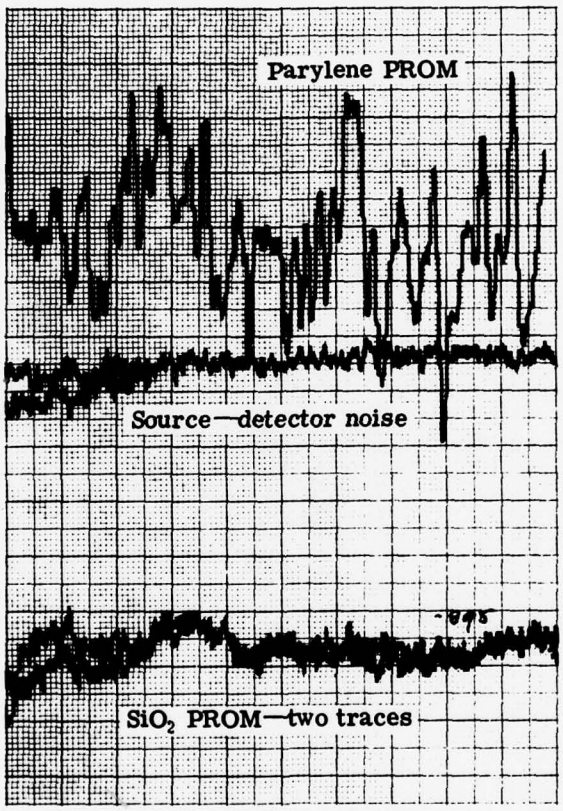

Figure 1-8 — Surface noise traces of Parylene- and SiO_2-coated PROMs

2. EXPERIMENTAL PROCEDURES

2.1 METHODS OF DEPOSITION

Most work was performed in a 6-inch Veeco pumping station equipped with a 24-inch water-cooled bell jar, quartz-iodine radiant substrate heaters, a micrometer valve for controlled oxygen bleed, a four-hearth Airco Temescal electron beam gun, and an optical monitor. In a typical deposition procedure, the chamber was evacuated to the low 10^{-6} Torr range. The substrate heaters were then turned on to heat the substrates slowly (8 °C/minute) to 250 °C. Some outgassing occurred and the system was allowed to stabilize back to the low 10^{-6} Torr range. Oxygen was then introduced at a controlled rate to a position slightly below the substrates, permitting the evaporated material to oxidize readily as it passed through the oxygen. Typical pressures during evaporation were 2×10^{-4} Torr. Thicknesses were measured using an optical monitor. The monitor consists of a quartz-iodine lamp focused on a Bausch & Lomb monochromator. The optical beam is chopped, introduced into the vacuum chamber, and focused onto a monitor slide. The reflected beam is split off be a beam splitter and is directed through a narrow pass filter to a silicon photodetector. The output signal from the photodetector is fed through a lock-in amplifier and displayed on a chart recorder. Typical monitor/wavelength was 543 nanometers. At the completion of the evaporation the substrate heaters were slowly turned down. After the heaters were turned off, the substrates were allowed to dynamically cool to ambient temperature before the system was vented.

Some work was also performed in a larger chamber. This system is 72 inches in diameter, and has a source-to-substrate distance of 60 inches. It is equipped with a two-hearth Airco-Temescal electron beam gun, substrate heaters, a controlled oxygen bleed valve, an optical monitor, a residual gas analyzer for detecting small amounts of gaseous impurities during evaporation, and provisions for glow discharge cleaning in situ immediately before deposition.

Evaporation procedures were essentially the same in both systems. Substrate temperature was more easily controlled in the larger system. The greater source-to-substrate distance and increased internal area of the larger system also permitted better deposition control. However, this system required long pump down cycles for evaporations in the 10^{-6} Torr range, and thus was unsuitable for continuous use in performing fast turnaround in a research program of this type.

2.2 METHOD OF SPUTTERED DEPOSITION

During the latter stages of the program, a few films were deposited using an ion beam sputtering system from Ion Physics Corporation. Although it was antiquated, this system allowed us to study two types of films: SiO_2 and Al_2O_3. Unlike conventional rf and dc sputtering, ion beam sputtering makes use of high-intensity focused ion beams in which a very intense plasma is generated in an auxiliary chamber. This plasma then diffuses into the main sputtering chamber. By

making use of a strong auxiliary magnetic field, the plasma emerges as a narrow beam. Additional voltage is applied at the target, where the ions receive the final energy required to perform sputtering. It was very difficult to control this system, and no monitoring was available.

2.3 MEASUREMENT TECHNIQUES

Three basic electrical measurements were made on these films. The first measurement was dielectric breakdown. Whenever a coating showed a high dielectric breakdown, its capacitance and I-V characteristics were also measured.

Dielectric breakdown measurements were made using a Northeast Scientific 6-kilovolt power supply and an RCA calibrated VTVM coupled through a voltage divider network, which provided a current limit when breakdown occurred. The voltage on the sample was increased in increments of 50 volts and allowed to stabilize for several seconds at each step. For this test, the breakdown field was defined as the highest field that the coating would sustain rather than the voltage at which failure occurred. These values were found to be reproducible within 10 percent for all the coatings studied.

For all measurements, samples were held in the mount shown in Figure 2-1. A spring-loaded indium pad provides a contact to the conductive electrode on the glass substrate. The top contact is a mercury coated pin, which produces a uniform mercury electrode with an area of 0.35 square centimeters. This method is much easier to implement than the technique of evaporating a metal on the coating. However, the mercury coated pin can produce erroneous readings if the mercury surface is contaminated. This contamination appears in the capacitance measurement as an anomalously small reading and hence is easily identified. But even under the best conditions, the data shows significant scatter.

Capacitance and I-V characteristics were measured by evaporating small aluminum pads on the samples, and then making contact with a metal probe (see Figure 2-2). Aluminum was chosen for the pads because the samples were expected to be n-type, and it was desired to achieve as nearly ohmic behavior as possible at that surface. Other (blocking) contacts (e.g., gold) may have yielded more consistent data, but the intent of the measurement is to look at the sample film and its contact with the In_2O_3 electrode only.

I-V characteristics were measured in the same manner as the breakdown fields. Most of the same equipment was also used, but the limiting resistor was replaced with a Kiethley picoammeter and voltage was held below 10 percent of the breakdown voltage to avoid possible damage to the picoammeter, which was not protected with a current limiter. Capacitance was measured directly, using a Boonton Electronics capacitance meter. For this measurement, all power supplies, meters, etc., were disconnected, and low capacitance leads (approximately 10 picofarads) were used to avoid erroneous data.

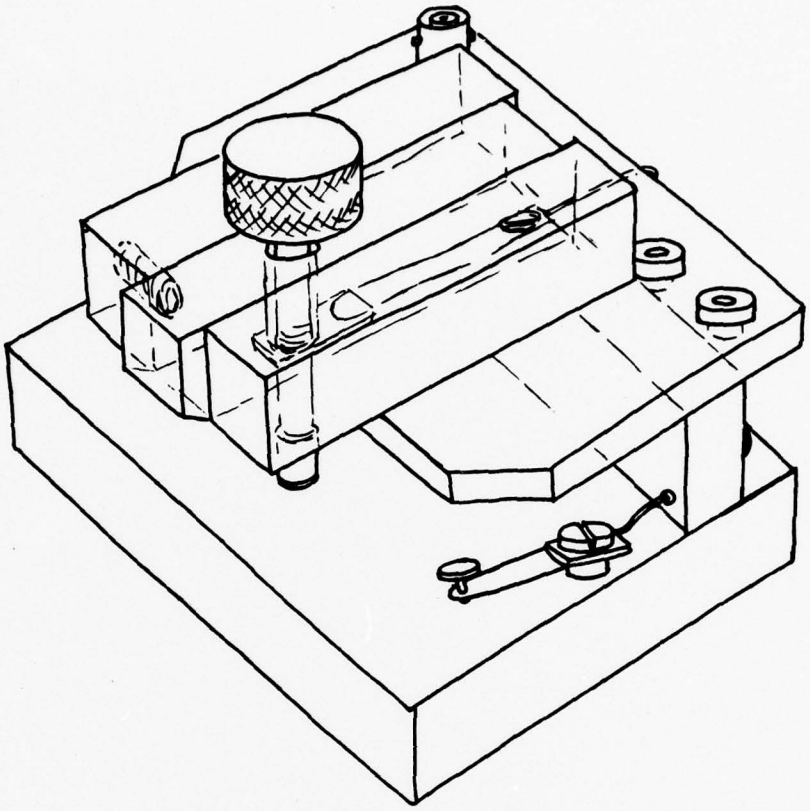

Figure 2-1 — Dielectric breakdown tester

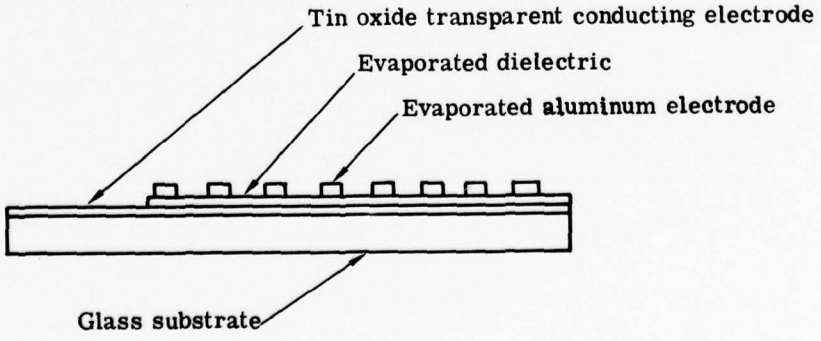

Figure 2-2 — Sample configuration for I-V and capacitance measurements

3. EXPERIMENTAL RESULTS

3.1 MATERIALS: SINGLE LAYER COATINGS

A number of oxides were chosen based on their published bulk properties. The oxides selected were SiO_2, Al_2O_3, Ta_2O_5, ZrO_2 and TiO_2. This selection provided a wide range of dielectric constant ($3 < E < 89$), and a range of refractive indices that allow design of multilayer dichroics. All the materials except Ta_2O_5 are commonly used in thin film coatings; hence, their deposition parameters could be readily established.

All films were deposited by electron beam evaporation. This deposition technique was chosen since it is well understood, and it gives repeatable optical properties. In addition, a great deal of data on the deposition of optical coatings of oxides by electron beam evaporation is available.

3.1.1 Materials: Al_2O_3

Aluminum oxide (Al_2O_3) was chosen first because it would triple the dielectric constant of the blocking layer. It also is easily deposited by electron beam evaporation, it can be deposited clear without post oxidation, and it has a high breakdown strength. The substrates were tin-oxide-coated glass (to determine deposition parameters) and $Bi_{12}SiO_{20}$ wafers polished on both sides.

The Al_2O_3 was easily deposited onto the glass substrates. A 4-micrometer film was very clear and had a breakdown voltage greater than 3,400 volts. The material was then deposited onto $Bi_{12}SiO_{20}$ substrates. These substrates were first heated to 250°C, then 4 micrometers of Al_2O_3 were deposited and the substrates were allowed to cool slowly. Inspection of the coated substrates revealed that the film had fractured. Closer examination revealed that where the film had fractured and pulled away from the substrate, part of the substrate had been pulled away with it. Although the adherence of the Al_2O_3 film to the $Bi_{12}SiO_{20}$ substrate was excellent, the high thermal expansion of the $Bi_{12}SiO_{20}$ and the high level of internal stress in the Al_2O_3 film caused crazing during cooldown. Because the only apparent solution to this problem is the use of multilayer, Al_2O_3 was removed from consideration as a dielectric coating although breakdown fields as high as 8.9×10^6 V/cm and dielectric constants of 8.4 were measured.

3.1.2 Materials: Ta_2O_5

Ta_2O_5 was of particular interest because of its high dielectric constant 24 and because it is frequently used as a dielectric in the thin film capacitor industry. Initially the substrates were 2 1/4- × 1 1/4- × 1/8-inch tin-oxide-coated glass. Three substrates were used during each run. A number of runs were made by evaporating stoichiometric tantalum pentoxide (Ta_2O_5). It was quickly found that a high degree of disassociation occurs during deposition, even when the oxygen bleed pressure is at the maximum of the system. The films ranged in color from light gray to dark gray; however, they were readily oxidized in air at approximately 200°C.

Figure 3-1 shows a time-temperature plot for complete reoxidation of 4.5-micrometer Ta_2O_5 films. Times for other coating thicknesses can be approximated by multiplying values on this plot by the ratio of actual coating thickness to the 4.5-micrometer standard. Experiments showed that Ta_2O_5 was readily formed when the Ta_2O_X films were placed in an oven at approximately 250°C, and then allowed to oxidize in air for 1-1/2 hours. However, lower temperatures for longer times also could be used.

Although the films appeared to have identical optical properties, variations in dielectric breakdown were observed that probably can be attributed to variations in oxidation and deposition conditions. The films were transparent and very hard after oxidation. The breakdown voltages were mostly in the vicinity of 1,500 volts, and the dielectric constants, E, were approximately 42. One run, however, showed extremely high breakdown voltage (3,400 volts) and E equal to 42. But this run could not be reproduced, and the mechanism that produced this breakdown strength cannot be explained.

Several runs were made using $Bi_{12}SiO_{20}$ as substrates. The substrates were coated on both sides with about 6-micrometers of Ta_2O_5. The initial side of the substrate could be coated without difficulty. When the substrate was turned over to coat the second side, however, the film on the first side crazed and flaked. This probably was caused by the high thermal expansion of the substrate during cycling, and by the bending due to nonuniform heating during the coating of the second side. This problem probably could be solved by using substrate rotation to simultaneously coat both sides. However, the substrates still must be cycled at 200°C to 250°C in air to oxidize the deposited films.

Figure 3-2 shows current-voltage (I-V) plots produced when aluminum pads were used for top electrodes as shown in Figure 2-2. When the voltage polarity was plus to minus (i.e., plus aluminum pad to minus tin oxide) the plot showed a region greater than 60 volts where I was proportional to V. This indicated regions where the film exhibited ohmic behavior. Below 60 volts, the plot showed that I was proportional to V^2. This probably was due to space charge effects, indicating that the electrodes were injecting carriers.

When the polarity was reversed (minus to plus), the plot showed that I was proportional to V^2, again indicating a space charge effect. Although Ta_2O_5 appeared to be a very likely film to be used, our attention turned to other films because of the thermal problems encountered.

3.1.3 Materials: ZrO_2

Another material that showed great promise was zirconium dioxide (ZrO_2). ZrO_2 has been the standard high-refractive-index layer for broadband antireflection coatings for many years, but little information about its dielectric properties is available. ZrO_2 is difficult to evaporate in the small chamber since its vapor pressure is very low (10^{-4} Torr at 2200°C). High power levels are required, and temperature control becomes very difficult due to radiation heating of the substrates by the source. Therefore, the effect of substrate temperature became impossible to evaluate. However, little or no effect from substrate temperature had been observed in other materials. Because of the high power levels required, bursting or spitting of the source material became a problem during evaporation.

The properties of the film were outstanding. The material required no oxidation when deposited with an oxygen bleed of 1×10^{-4} Torr. The dielectric constant was 22, and the breakdown voltage for a 1.5-micrometer-thick film was 1,500 volts. Again, the film was initially deposited on tin-oxide-coated glass substrates to determine the evaporation parameters.

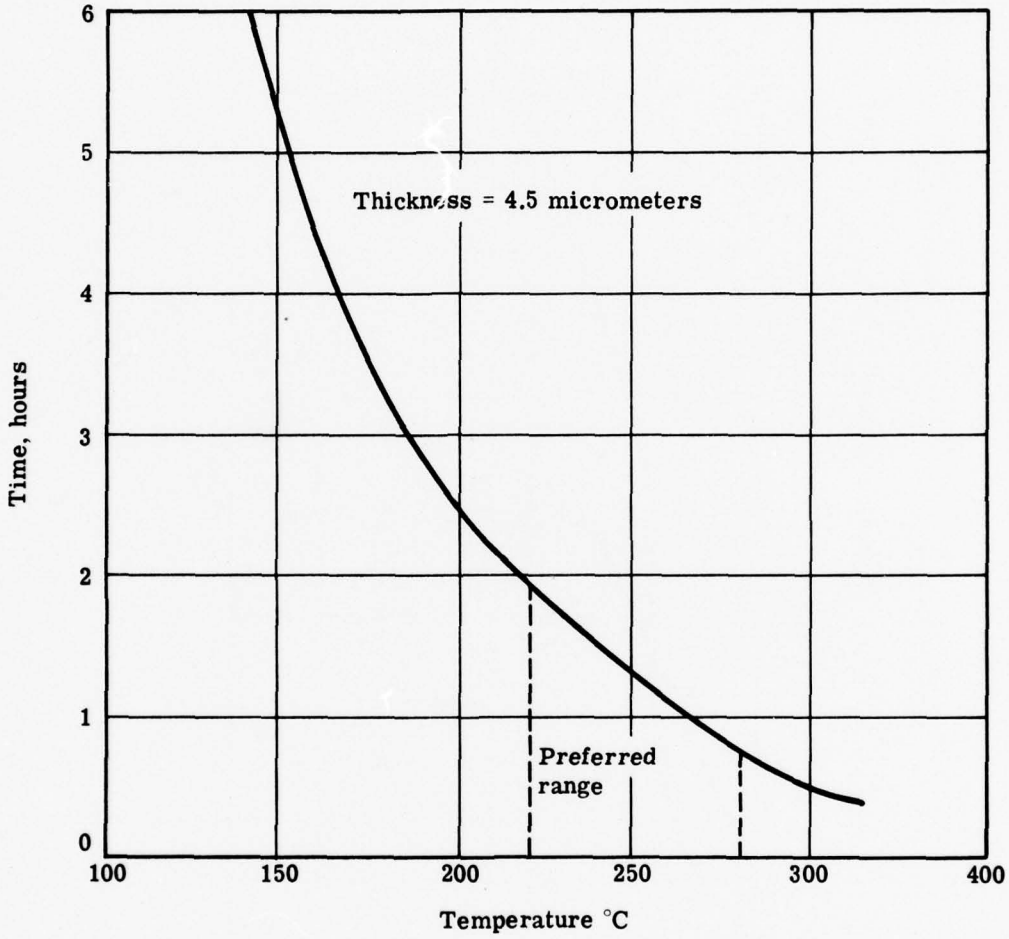

Figure 3-1 — Baking time in air for Ta_2O_5 films

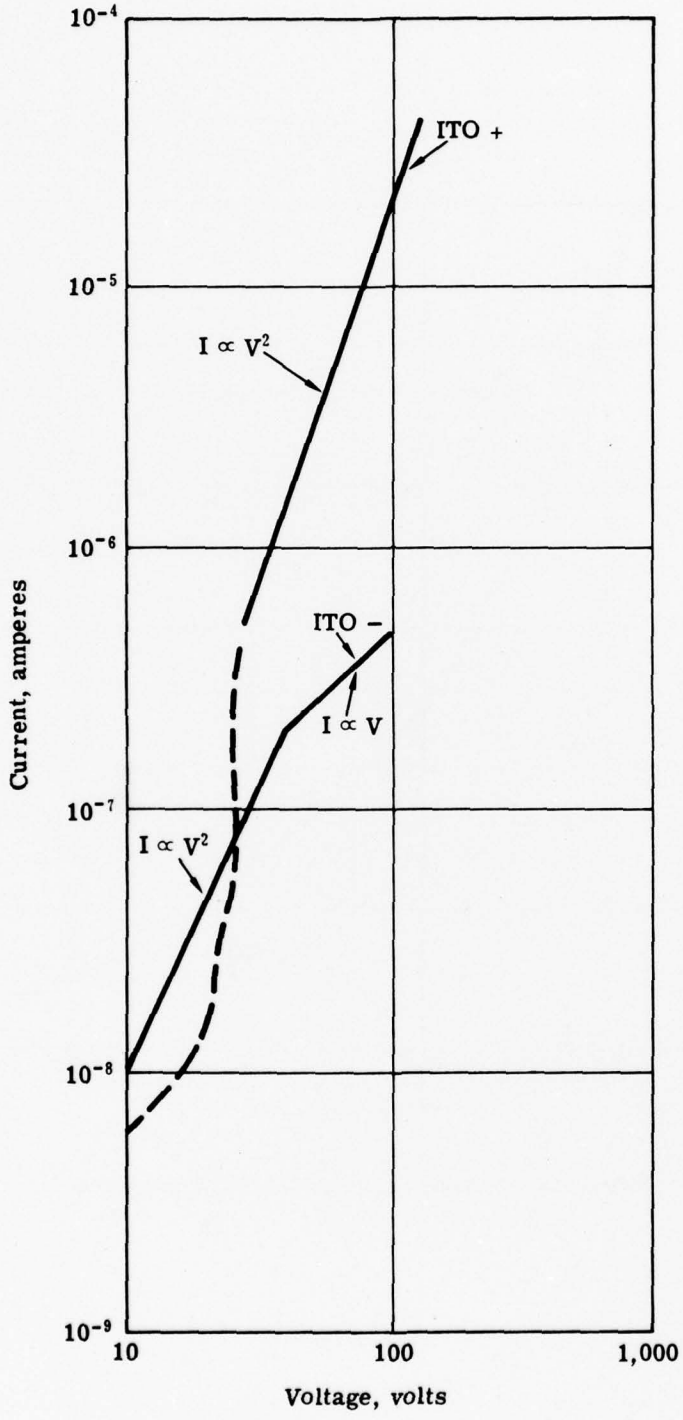

Figure 3-2 — I-V characteristic of Ta_2O_5 film

Several runs then were made on $Bi_{12}SiO_{20}$ substrates. The same problems encountered with Ta_2O_5 films on $Bi_{12}SiO_{20}$ substrates were experienced. For the ZrO_2, however, the films fractured during cooling after deposition onto the first side. To prove that this phenomena was not a problem specific to the small vacuum chamber, $Bi_{12}SiO_{20}$ substrates were coated in a larger vacuum chamber. This chamber had a longer source to substrate distance, and provided better control of substrate temperature because of the elimination of substrate heating due to source radiation. Again, the film fractured during cooling after deposition.

Typical deposition rates were 20 angstroms per second, although slower rates were used (1 to 5 angstroms per second) to see whether more oxidation of the films during evaporation would improve breakdown voltage and adhesion to $Bi_{12}SiO_{20}$, and increase dielectric constant. However, no improvements were observed. Rates greater than 20 angstroms per second were attempted, but these rates resulted in excessive bursting from the source. Samples were placed in an oven at 400℃ and oxidized in air for 2 hours. No changes from the properties of the as-deposited coatings were observed. However, the large thermal expansion of the $Bi_{12}SiO_{20}$ again created too much stress to allow the evaporated film to adhere.

Figure 3-3 shows I-V plots for evaporated ZrO_2 using vacuum-deposited aluminum pads as shown in Figure 2-2. When the polarity was plus to minus (i.e., plus aluminum to minus tin oxide), I was proportional to V above 30 volts. This indicated ideal I-V characteristics where the film behaved ohmic. At values greater than 30 volts, I was proportional to V^2, indicating carrier injection. When the polarity was reversed, the plot showed that I was proportional to V^2, again indicating a space charge effect.

3.1.4 Materials: SiO_2

Silicon dioxide (SiO_2) was considered because it has both a low dielectric constant and a low refractive index, and because a comparison with previously available data was desired. Sputtered coatings have been found to have a breakdown field greater than 2×10^6 volts per centimeter and 6-micrometer layers deposited at 350℃ were adherent to $Bi_{12}SiO_{20}$. However, evaporated coatings exhibited breakdown fields no better than 0.8×10^6 volts per centimeter, and 4-micrometer coatings peeled off the $Bi_{12}SiO_{20}$ as soon as the crystals were temperature-cycled to 150℃. No improvement was obtained for oxygen bleed pressures as high as 2×10^{-4} Torr and substrate temperatures up to 250℃. Post baking in air had no effect on the breakdown. The failure is believed to have been caused by the inherent porosity of electron-beam-evaporated SiO_2. The film is very slightly hygroscopic, and absorbs sufficient moisture to break down at very low voltages.

3.2 MATERIALS: MULTILAYER FILMS

Multilayer films were attempted to eliminate stresses created when thicker single layer films were deposited on hot $Bi_{12}SiO_{20}$ substrates. It was believed that depositing alternate $\lambda/4$-thick dielectric films of certain materials would eliminate the thermal expansion problem usually encountered when Ta_2O_5 and ZrO_2 are deposited because the thin films would be able to stress relieve during deposition and cooling.

3.2.1 Multilayer Coatings Design

Figures 3-4 and 3-5 show typical coating designs used for the multilayers and the configuration of the layers. Figure 3-4 shows a low-pass design of a 21-layer SiO_2/ZrO_2 film on a $Bi_{12}SiO_{20}$ substrate, with a 0.6-micrometer indium oxide (9-percent tin oxide) sputtered, transparent, conductive electrode. Figure 3-5 shows a high-pass design curve of a 21-layer ZrO_2/SiO_2 film on a $Bi_{12}SiO_{20}$ substrate, with a 0.6-micrometer indium oxide (9-percent tin oxide) sputtered, transparent, conductive electrode. As these figures also show, the low-pass and high-pass coatings are identical except for the ordering of their SiO_2 and ZrO_2 layers. The transmission/reflection curves of these multilayers are shown in Figures 3-6 and 3-7.

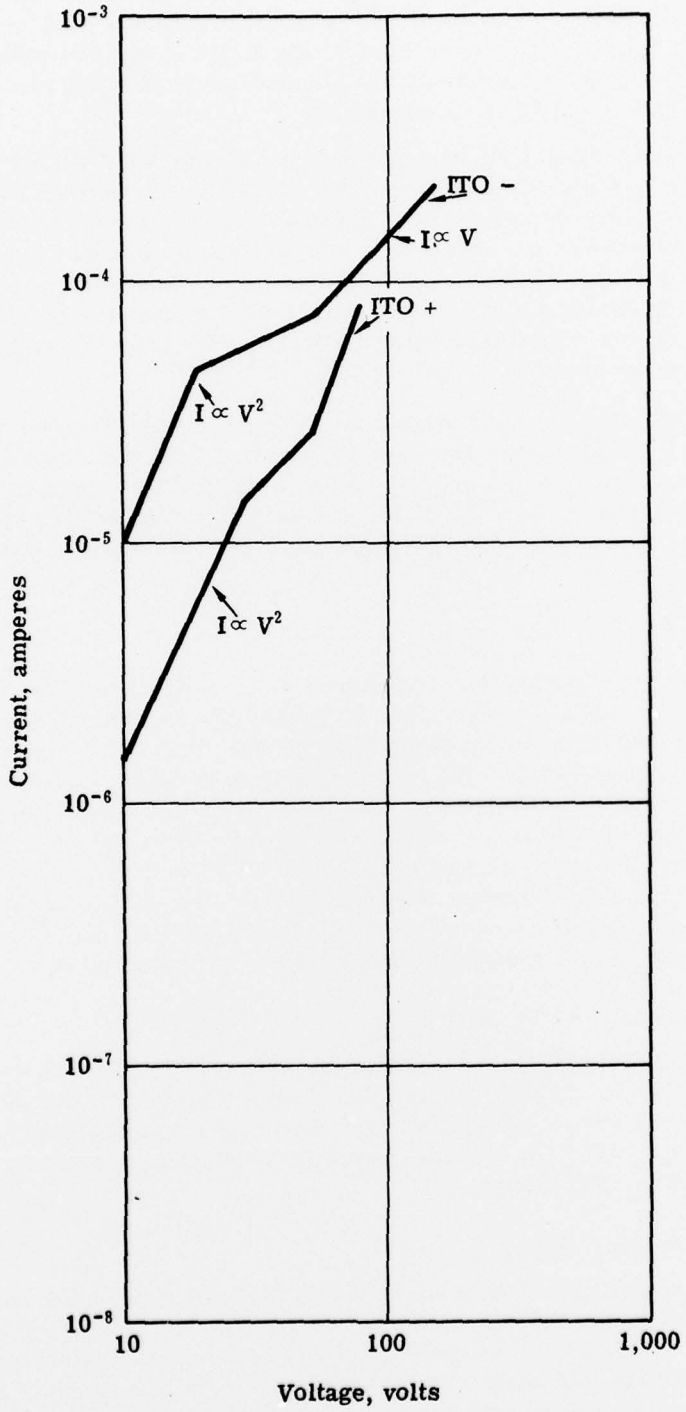

Figure 3-3 — I-V characteristic of ZrO_2 film

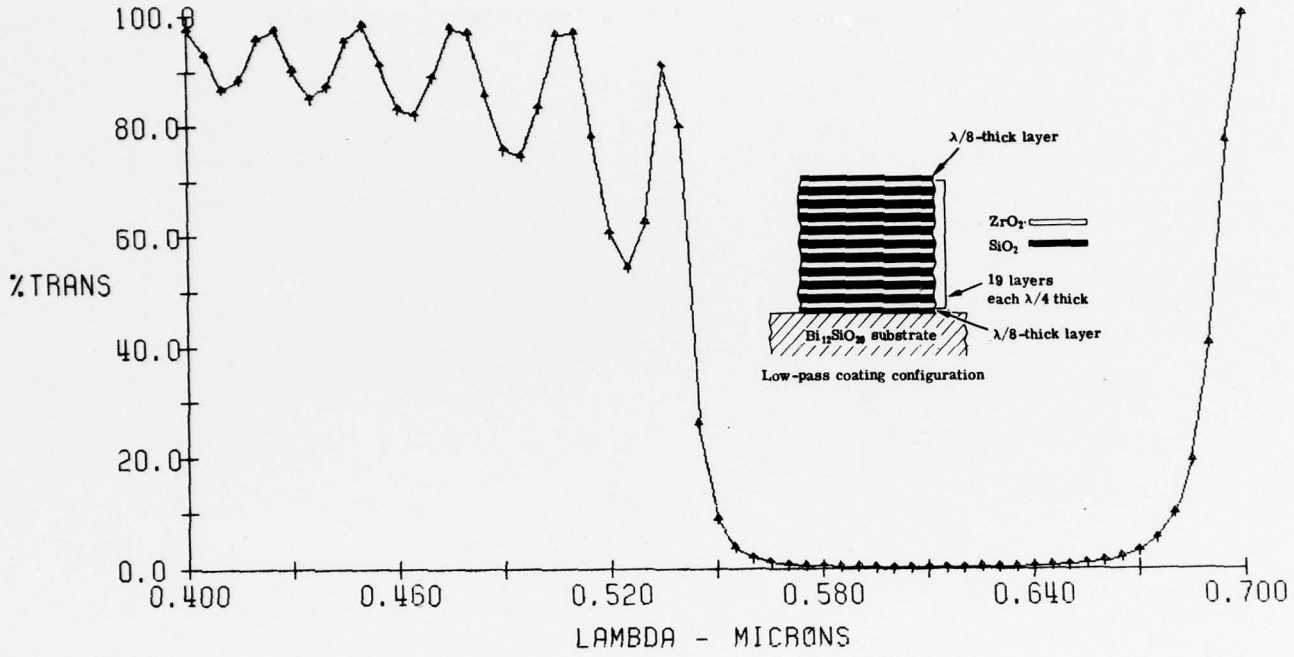

Figure 3-4 — Coating design for a low-pass SiO_2/ZrO_2 multilayer

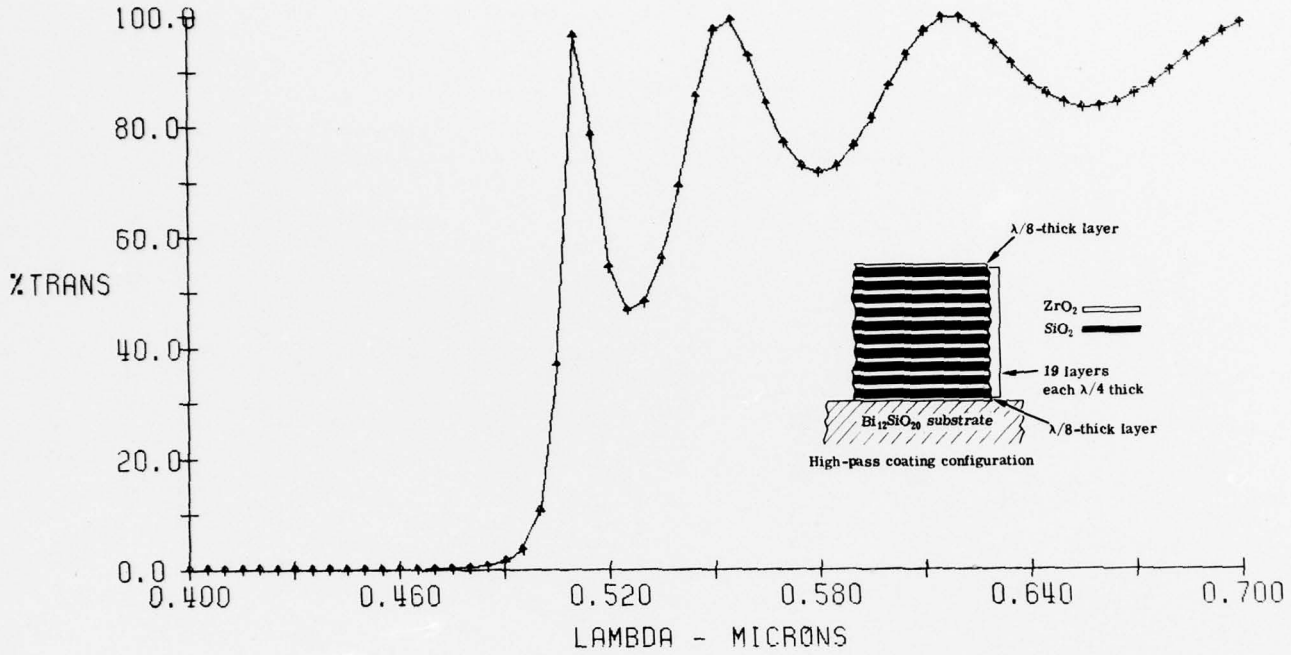

Figure 3-5 — Coating design for a high-pass ZrO_2/SiO_2 multilayer

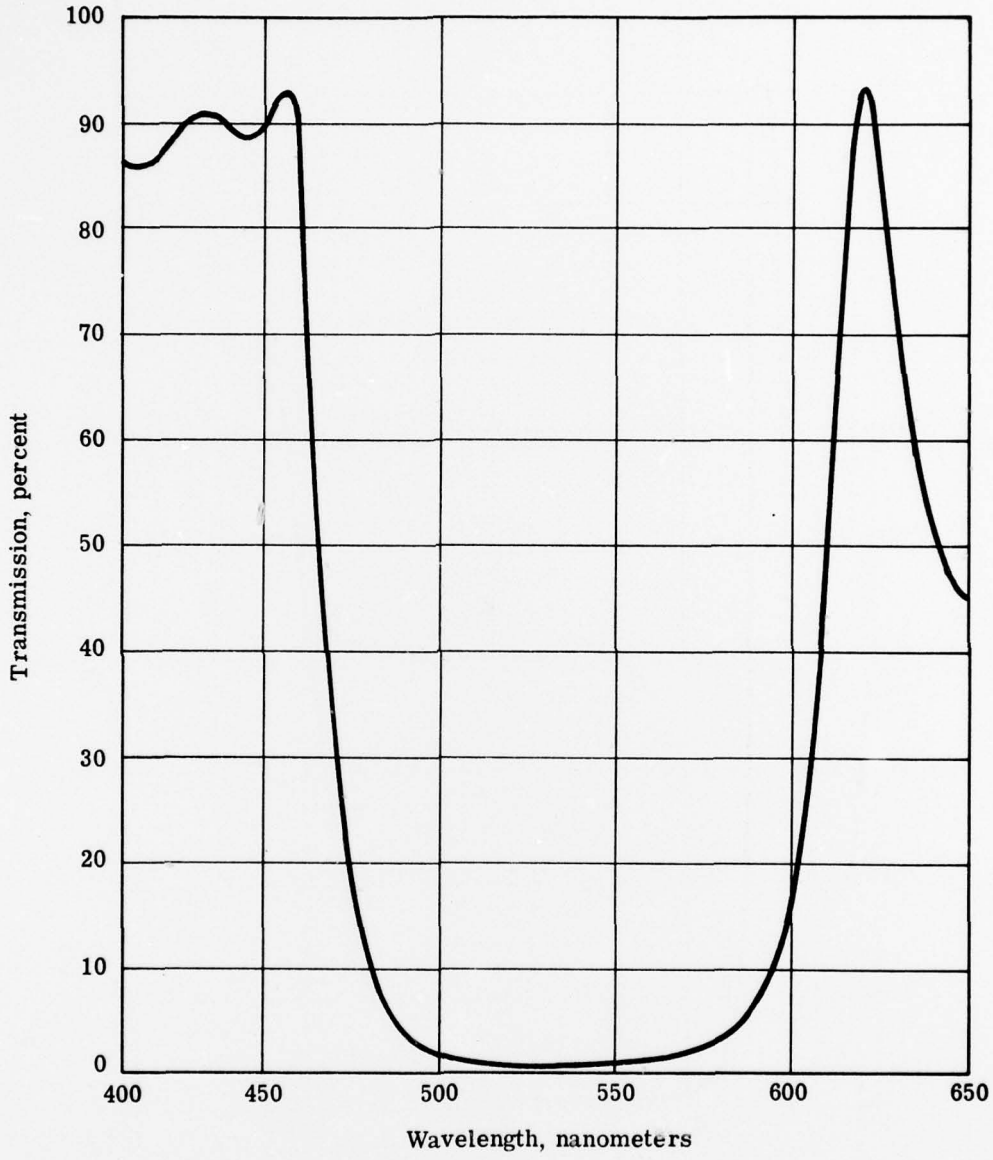

Figure 3-6 — Low-pass transmission of ZrO_2/SiO_2-coated PROM

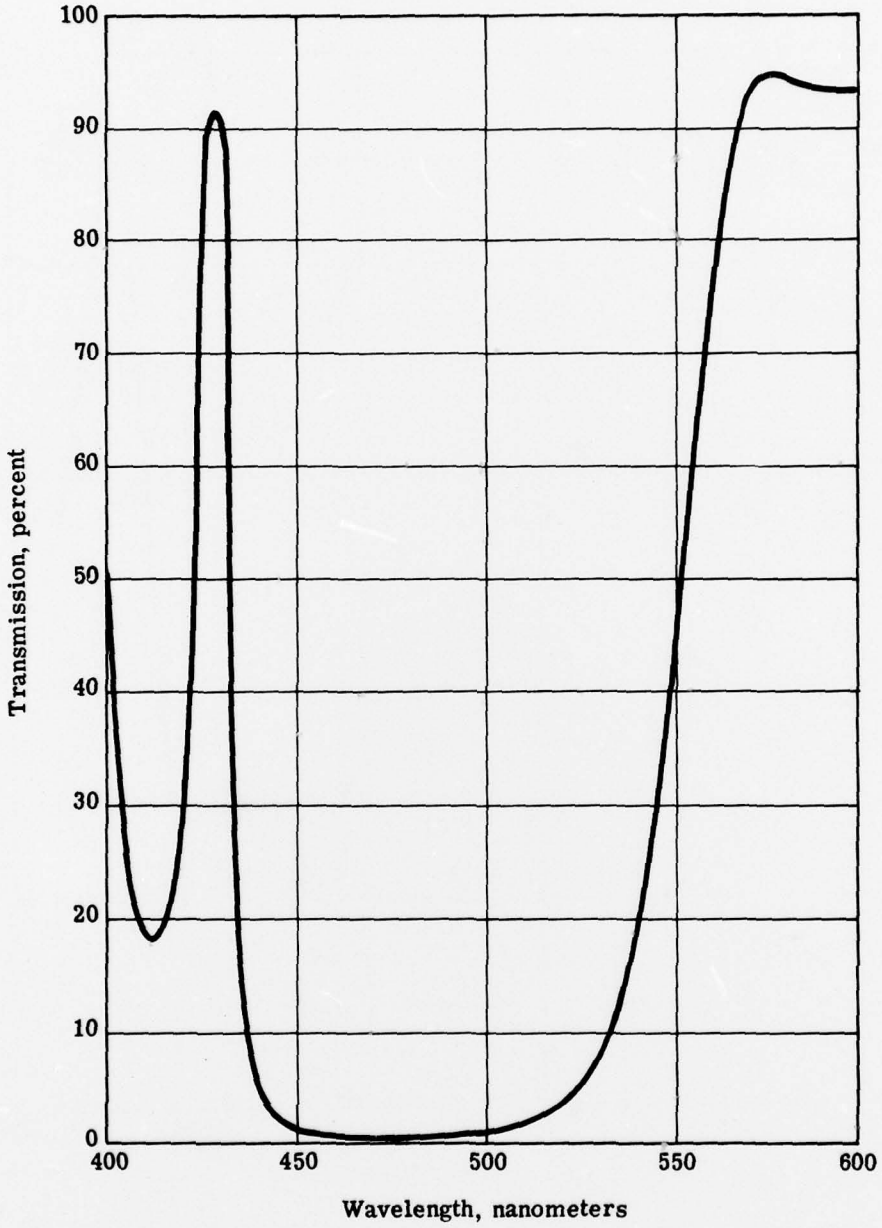

Figure 3-7 — High-pass transmission of ZrO_2/SiO_2-coated PROM

3.2.2 TiO_2/SiO_2 Multilayers

The first materials tried were titanium oxide (TiO_2) and silicon dioxide (SiO_2) in the small chamber on tin-oxide-coated glass substrates. A 15-layer TiO_2/SiO_2 film was deposited. Each layer was $\lambda/4$ thick. The resulting film was dark in color due to incomplete oxidation of the TiO_2 during evaporation, even though the oxygen bleed into the chamber was at 2×10^{-4} Torr. To turn the film clear, the substrate had to be baked in air at approximately 600°C. This temperature is higher than $Bi_{12}SiO_{20}$ (the ultimate substrate) would be able to withstand without surface damage after polishing.

The run was repeated in the large chamber, where the TiO_2 could be deposited clear. Although the resulting film was quite adherent and transparent, its dielectric strength was too low to be of any interest. Typical breakdown voltages were less than 500 volts and dielectric constants (E) were 5.5.

3.2.3 Ta_2O_5/SiO_2 Multilayers

The second series of films attempted was Ta_2O_5/SiO_2. A 15-layer film of alternating $\lambda/4$ thickness was deposited onto tin-oxide-coated glass substrates. The resulting film was slightly gray in color, but was easily oxidized in air at about 200 to 250°C. The film was 3 micrometers thick. It had a dielectric constant of 19, and a breakdown of 1000 volts. Because of the post baking needed to complete this multilayer, we decided to search for a film that could be deposited clear.

3.2.4 ZrO_2/SiO_2 and HfO_2/SiO_2 Multilayers

Zirconium dioxide/silicon dioxide (ZrO_2/SiO_2) and hafnium dioxide/silicon dioxide (HfO_2/SiO_2) multilayers were then attempted. Because of the high power levels needed to evaporate ZrO_2 and HfO_2, these multilayers were deposited in the large chamber. The multilayers were deposited onto $Bi_{12}SiO_{20}$ wafers, and adhered quite well. Electrodes were deposited onto the wafers, and electro-optic devices were made for testing the multilayer dielectric films.

3.3 SPUTTERED COATINGS

During the closing weeks of the program, two attempts were made to determine the advantages of sputtered coatings. First, it was shown that SiO_2 could be sputtered to yield a PROM with properties similar to the Parylene-coated device. An image of a bar target exposed on a PROM that is coated with SiO_2 is shown in Figure 3-8. Wafer quality is poor (note the large amount of birefringent strain visible), but the bar target is sharp. A test was also made of sputtered Al_2O_3, the only other target material available. The test was not completely successful in that there was light crazing of the coating, again due to internal stress in the film, but it was possible to fabricate a device. The result is shown in Figure 3-9. The contrast is low due to light scattered in the crazed coating, but the image appears to be sharp. No measurement of modulation has yet been made because of very severe scattering. This scattering makes observation of the high resolution portion of the bar target very difficult.

3.4 EXPERIMENTAL PROMS

HfO_2/SiO_2 PROMs did not function, possibly because the deposited film was only 0.9-micrometer and 1.0-micrometer on each side. Breakdown occurred at about 700 volts. More significantly, the I-V characteristic showed very high conductivity, indicating that no voltage division was occurring between the substrate and the blocking layer.

The ZrO_2/SiO_2 PROM did operate. The intention was to deposit a film on the first side that would transmit blue and reflect red (low pass), and to deposit a film on the second side that would transmit red and reflect blue (high pass).

1. Wafer quality poor
2. Observed resolution 80 lp
3. Sensitivity similar to 6-micrometer parylene

Figure 3-8 — Bar target exposure on a PROM with a sputtered SiO_2 coating

Figure 3-9 — Bar target exposure on a PROM with a sputtered Al_2O_3 coating

The deposited multilayers were 1.0-micrometer thick on each side. Breakdown occurred at 600 volts, and the dielectric constant was about 17. The breakdown was significantly lower than had been anticipated. The resolution was poor (see Figure 3-10), but the $Bi_{12}SiO_{20}$ wafer used to make the PROM was of poor quality and the polished surface had a transmitted wavefront greater than $\lambda/2$ rms. The capacitance of the ZrO_2/SiO_2 multilayers was about 5×10^{-10} farads, but I-V characteristics were very disappointing (see Figure 3-11). Again, vacuum-deposited aluminum pads as shown in Figure 2-2 were used as top electrodes. A minus to plus polarity produced a curve that showed I to be approximately proportional to V^2, again indicating a space charge effect. The resistivity was lower than what was expected of these materials. When the polarity was reversed, I became approximately proportional to V^4; this high variable nonintegral slope indicates a high density of traps and significant disorder in the film.

The peculiar results indicate that the electron-beam-evaporated films are not truly pure and do not exhibit bulk properties. The films apparently are incompletely oxidized, although they are being evaporated in a very high oxygen atmosphere. The optical properties are excellent, but the electrical properties are poorer than desired. An alternative method of depositing these films is rf sputtering. An rf-sputtered film can be deposited with increased stoichiometry when compared to vacuum evaporated films. In addition, higher purity layers are realized, more realistic bulk properties are attained. Reactive sputtered films are easier to control and duplicate than vacuum evaporated films.

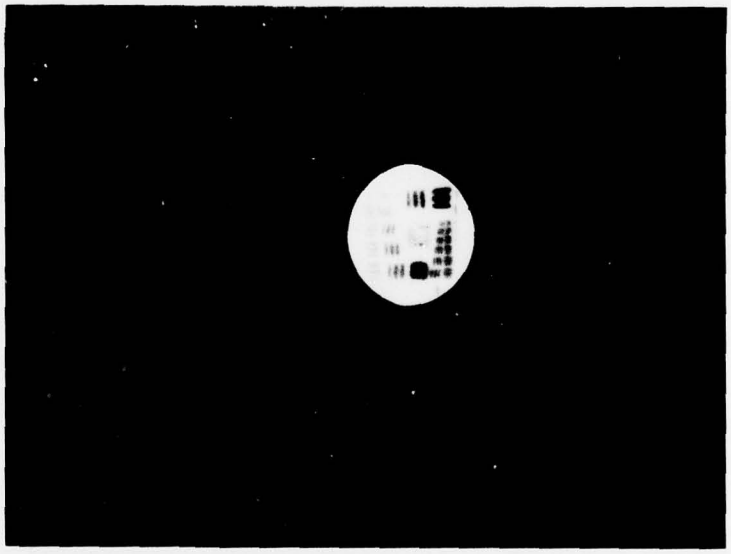

Figure 3-10 — Bar target exposure on a ZrO_2/SiO_2-coated PROM

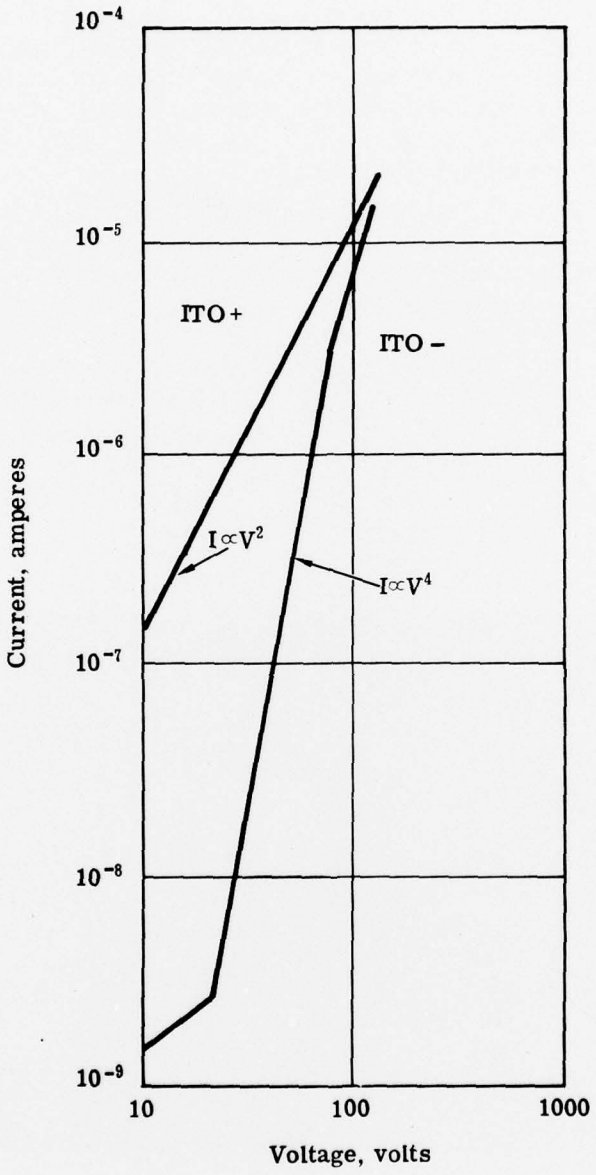

Figure 3-11 — I-V characteristic of ZrO_2/SiO_2 film

4. EVAPORATED INDIUM/TIN OXIDE COATINGS

In support of this program, Itek has used Internal Research and Development funds to study the feasibility of depositing indium tin oxide by electron beam. This coating is necessary for development of a fully integrated dichroic or antireflection coating for the PROM. The work has concentrated on extending previous Itek work in this area to fit conditions suitable for PROM fabrication.

The material chosen for this work was E. M. Merck's substance A, an indium tin oxide similar to the $In_2O_3/0.09\ SnO_2$ powder used in previous work. However, substance A is pelletized, and virtually eliminates spitting and loss of material from the crucible during heatup. The coatings were deposited on room-temperature Pyrex substrates and Parylene C substrates. Low substrate temperatures had to be used to prevent crystallization in the coating and its attendant scattering. (Crystallization occurs for substrate temperatures above 100°C.) Extremely high oxygen bleed pressures — up to 2×10^{-4} Torr with the bleed at the substrate surface — were used to maximize the oxidation. The as-deposited coatings were gray, indicating substantial amounts of InO due to incomplete oxidation. However, the coatings were hard and adherent. This represented a major improvement over earlier work in which the coatings at this stage were black and could be wiped off.

The coatings were then baked in air to complete oxidation. The black coatings had to be baked at 300°C for 2 hours to achieve complete conversion. However, the new gray coatings could be converted at temperatures as low as 125°C. Lower temperatures had no effect on the layers. It is significant that these coatings can be oxidized without crystallization occurring. Typically, a 0.36-micrometer coating baked at 150°C in air for 60 minutes exhibits a moderately stable sheet resistance of 1.2×10^4 ohms per square. This resistance can be reduced sharply by baking at 150°C in a moderate vacuum (about 10 Torr) for 2 hours. The sheet resistance then drops to roughly 500 ohms per square. This value drifts upward gradually when the sample is left at normal room temperature and stabilizes at 1100 ohms per square after approximately 300 hours.

5. RESULTS AND CONCLUSIONS

While several significant results were obtained on the program, it was found that the electron-beam-evaporated coatings did not have acceptable properties for use as blocking layers in the presence of high electric fields. It has been found that the trial coatings had completely acceptable optical properties, capacitance, and breakdown fields as long as charge injection was avoided (see Tables 5-1 and 5-2). With ohmic or injecting contacts, however, the coatings exhibited a high conductivity (about 10^{-4} amperes per square centimeter at 100 volts). The high conductivity and very nonlinear I-V curves are characteristic of materials having extremely high defect densities. As a secondary effect, the high conductivity permits lateral charge migration in the blocking layer resulting in blurred images. In addition, adhesion problems were encountered with the various coatings: none of the single-layer coatings would adhere to $Bi_{12}SiO_{20}$, and only multilayer coatings deposited in the large coating chamber were adherent. The 60-inch throw distance in the large coating tank effectively eliminated the substrate temperature nonuniformity due to radiant heating from the source; but in spite of this, single layer coatings did not stick. For these reasons, it was concluded that electron-beam-deposited coatings are not a viable method of depositing oxides despite their advantages in conventional optical coating.

During the final stages of the program, an attempt was made to evaluate sputtered coatings on $Bi_{12}SiO_{20}$. These results were extremely promising: the sputtered single layers of SiO_2 and Al_2O_3 had reasonable adhesion, and they exhibited none of the charge spreading observed with the evaporated coatings. Based on present results, sputtering is clearly the method that should be used for further development work.

Table 5-1 — Refined Breakdown Field Values

Material	Breakdown, volts per micrometer	Oxygen Pressure, Torr
SiO_2	110	10^{-4}
Ta_2O_5	1700	10^{-4}
ZrO_2	1100	10^{-4}
HfO_2	Will not adhere in thick layers	10^{-5}
Ta_2O_5/SiO_2	350	10^{-5}
ZrO_2/SiO_2	480 (thick: 1.2 micrometers or thicker)	10^{-5}
	~6000 (thin: approximately 0.5 micrometer)	10^{-5}
HfO_2/SiO_2	850	10^{-5}
TiO_2/SiO_2	400 (thick: 1.0 micrometer or thicker)	10^{-4}
	shorten (thin: less than 0.5 micrometer)	10^{-4}
Al_2O_3/ZrO_2	Pinholes — no measurement possible	10^{-4}

Table 5-2 — Refined Dielectric Constants

Material	Dielectric Constant (E)
Ta_2O_5	43
ZrO_2	22
Ta_2O_5/SiO_2	19
ZrO_2/SiO_2	15
HfO_2/SiO_2	11
ZrO_2/Al_2O_3	23 (very thin Al_2O_3 layers)

6. SUGGESTIONS FOR FURTHER WORK

It is advisable to continue this program, but with a different approach. Instead of electron beam deposition, sputtering should be employed. With some exceptions, the same materials should be used. The criteria for selection of these materials have not changed: each material should have a dielectric constant between 10 and 60, and should have a high bulk resistance and a high dielectric breakdown field.

Use of sputtering in combination with these materials will permit interesting and potentially fruitful comparisons between the properties of electron-beam-deposited coatings and the properties of sputtered coatings. It will also serve as a basis for development of an advanced PROM.

It is also suggested that an attempt be made to sputter $Bi_{12}SiO_{20}$ as a blocking layer. As its main advantage over other films, sputtered $Bi_{12}SiO_{20}$ has optical properties identical to those of the crystal substrate. However, very little is known about the dielectric strength of $Bi_{12}SiO_{20}$ or its electrical properties at high electric fields.